

Loss of Claudin-15, but Not Claudin-2, Causes Na⁺ Deficiency and Glucose Malabsorption in Mouse Small Intestine

ATSUSHI TAMURA,* HISAYOSHI HAYASHI,† MITSUNOBU IMASATO,* YUJI YAMAZAKI,* ASUKA HAGIWARA,* MASAMI WADA,* TETSUO NODA,§ MITSUHIRO WATANABE,|| YUICHI SUZUKI,‡ and SACHIKO TSUKITA*

*Laboratory of Biological Science, Graduate School of Frontier Biosciences and Graduate School of Medicine, Osaka University, Yamadaoka, Suita, Osaka;

†Laboratory of Physiology, School of Food and Nutritional Sciences, University of Shizuoka, Shizuoka; ‡Department of Cell Biology, Cancer Institute of Japanese Foundation for Cancer Research, Ariake, Koto-ku, Tokyo; and §Department of Internal Medicine, School of Medicine, Keio University, Tokyo, Japan

BACKGROUND & AIMS: In the small intestine, the paracellular transport of Na⁺ is thought to be critical for luminal Na⁺-homeostasis and the transcellular absorption of nutrients by Na⁺-driven transporters. Na⁺ is supplied to the intestinal lumen from the submucosa and serum through tight junctions, which form a paracellular barrier between the cells of epithelial sheets. However, the molecular basis for this paracellular transport of Na⁺ is not well understood. Here, we examined this mechanism by performing loss-of-function studies of claudin-2 and claudin-15, two tight-junctional membrane proteins that are specifically and age-dependently expressed in the villi and/or crypts of small intestinal epithelia. **METHODS:** Knockout mice for claudin-2 or claudin-15 were subjected to histologic, cell biologic, electrophysiologic, and physiologic analyses. **RESULTS:** Examination of the knockout mice revealed that both claudin-2 and claudin-15 play crucial roles in the transepithelial paracellular channel-like permselectivity for extracellular monovalent cations, particularly Na⁺, in infants and adults. Especially in *Cldn15*^{-/-} adults, the luminal Na⁺ concentration in the small intestine measured directly in vivo was abnormally low, and glucose absorption was impaired, as assessed by the oral glucose tolerance test and estimation of unabsorbed glucose. **CONCLUSIONS:** We propose that the “Na⁺-leaky” claudin-15 is indispensable in vivo for the paracellular Na⁺ permeability, luminal Na⁺-homeostasis, and efficient glucose absorption in the small intestine, but claudin-2 is indispensable for only the first of these functions. Claudin-15 knockout leads to Na⁺ deficiency and glucose malabsorption in the mouse adult small intestine.

Keywords: Tight Junction; Na⁺-Homeostasis; Glucose Absorption.

The small intestine is responsible for nutrient absorption, and the absorption of many kinds of nutrients, including monosaccharides, amino acids, and vitamin C, is coupled directly to Na⁺ absorption.^{1–3} Tight junctions are thought to form the specific paracellular route by which Na⁺ is supplied across epithelia from the submucosa and serum to the intestinal lumen, although the

molecular bases for this transport remain to be elucidated.^{4–7} Epithelial tight junctions form the belt-like cell-cell adhesion structure known as the *zonula occludens* (zTJ), which has a paracellular barrier function with permselectivity. Electrophysiologic studies show that the paracellular routes for ions through zTJs across the small intestinal epithelial sheets are highly permeable to extracellular ions, with a high selectivity for Na⁺ and K⁺, compared with Cl⁻.^{6–11}

Claudin family members are required for zTJ formation. Claudins have molecular masses of around 23 kilodaltons and 4 transmembrane domains; they comprise a multigene family of at least 24 members in mice and humans.^{12–16} The idea that claudins determine not only the barrier function of zTJs but also the paracellular permeability across epithelial cell sheets has been substantiated in cultured cells, by transfection and knockdown experiments.^{13,17–21} The conductance-increasing “leaky” claudins permit epithelial cell sheets to be permeable to monovalent and/or divalent cations and/or anions. Among these claudins, claudin-2 and claudin-15 are unique in increasing epithelial permeability to monovalent cations when exogenously expressed, and their knockdown has the opposite effect in cultured epithelial cells.^{17,19,21–23} Furthermore, studies in humans bearing claudin mutations and gene-knockout studies in mice have revealed specific roles for several types of claudins in the zTJ-barrier or its selective ion permeability and in related pathologic phenotypes.^{24–34}

Previous studies have determined that various types of claudins, claudins-1/2/3/4/5/7/8/12/15/20/22/23, are involved in zTJ-structure and functioning.^{13,14,16,33,35,36,37} Here, we analyzed knockout mice for claudin-2 or claudin-15, tight-junctional membrane proteins of the small intestinal epithelia. Both claudins were responsible for the transepithelial paracellular permeability to extracel-

Abbreviations used in this paper: IBD, inflammatory bowel disease; Isc, short circuit current; IPGTT, intraperitoneal glucose tolerance test; OGTT, oral glucose tolerance test; qRT-PCR, quantitative real-time polymerase chain reaction; zTJ, zonula occludens.

© 2011 by the AGA Institute

0016-5085/\$36.00

doi:10.1053/j.gastro.2010.08.006

lular monovalent cations, especially Na^+ , with some differences between infants and adults; we therefore characterized them as intestinal “ Na^+ -leaky” claudins. Our findings in the adult small intestine indicate that claudin-15, but not claudin-2, is essential for luminal Na^+ -homeostasis in vivo, which is required for glucose absorption. Although the *Cldn15*^{-/-} megaintestine phenotype compensates to some extent for the claudin-15 deficiency-induced defects in glucose absorption, defective glucose absorption was still detectable in the small intestine of adult claudin-15-deficient mice. Because glucose is absorbed at the apical intestinal membranes by an Na^+ -driven glucose transporter, Na^+ -glucose transporter1 (SGLT1), our findings reveal a close physiologic relationship between claudin-15-based paracellular Na^+ transport and the transcellular transport of Na^+ and glucose in intestinal epithelial cells.

Materials and Methods

Animals

Claudin-2- and claudin-15-deficient mice were generated in Shoichiro Tsukita's laboratory^{33,34} and given by Shoichiro Tsukita to Sachiko Tsukita and Tetsuo Noda. All animal experiments were performed in accordance with protocols approved by the Osaka University School of Medicine Animal Studies Committee.

Antibodies

The following antibodies were used: rabbit polyclonal anti-claudin-2, anti-claudin-15, and anti-ZO-1; rat monoclonal anti-occludin,^{33,38} anti-claudin-3 (Zymed Laboratories, San Francisco, CA), and anti-E-cadherin (a kind gift from M. Takeichi, CDB, Kobe, Japan); rabbit anti-NHE3 (a kind gift from S. Grinstein, The Hospital for Sick Children, Toronto, Canada); fluorescein isothiocyanate-labeled goat anti-rabbit immunoglobulin G and cy3-labeled goat anti-rat immunoglobulin G (Jackson Laboratory, Bar Harbor, ME). Rhodamine-phalloidin was from Cytoskeleton (Denver, CO).

Quantitative Real-Time Polymerase Chain Reaction

Quantitative real-time polymerase chain reaction (qRT-PCR) was performed as described previously.^{33,39}

Immunofluorescence Microscopy

Mouse intestine was dissected and frozen in liquid N_2 . Frozen sections were cut and processed for indirect immunofluorescence microscopy as described previously.^{33,38}

H&E Staining

The small intestine and colon were fixed as “Swiss rolls” for H&E staining.

Freeze-Fracture and Scanning Electron Microscopy

The samples were processed for freeze-fracture and scanning electron microscopy as previously described.³²

Electrophysiologic Measurements

The middle one-third of the small intestine (jejunum) was isolated. After the musculature was removed by blunt dissection, the distal part of the jejunum was mounted as a flat sheet between 2 Ussing chambers, with an exposed-area of 0.2 cm^2 (for adult intestine) or 0.03 cm^2 (for infant intestine) to examine the transepithelial conductance and NaCl dilution potential and bi-ionic potential.^{9,23} The glucose-dependent short circuit current (Isc) was estimated as described in detail in Supplementary Materials and Methods.

Ion and Glucose Concentration of Small Intestinal Contents

The contents of the small intestine were collected from mice. In most cases, the wet and dry weights of the material were measured to obtain its water content. The samples were then resuspended in water and centrifuged to obtain the supernatant. The $[\text{Na}^+]$ and $[\text{K}^+]$ were measured using an ion meter, and the glucose concentration was determined using the glucose oxidase method.

Transmural Leakage of Na^+ and K^+ From the Inverted Small Intestinal Sac In Vitro

The middle one-third of the small intestine was obtained from 8- to 16-week-old adult *Cldn15*^{-/-} mice and their control wild-type littermates. The inner surface of the gut segment was inverted to measure the permeability of Na^+ and K^+ .

Oral Glucose Tolerance Test and Intraperitoneal Glucose Tolerance Test

Oral glucose tolerance test (OGTT) and intraperitoneal glucose tolerance test (IPGTT) were performed using standard protocols (see Supplementary Materials and Methods).

Estimation of Glucose-Dependent Isc

The glucose-induced, SGLT1-based phlorizin-inhibited Isc in wild-type small intestine was estimated by using Ussing chamber (see Supplementary Materials and Methods).

Statistical Analysis

Data were expressed as means \pm standard error of mean. The statistical significance of the difference between 2 groups of data was evaluated by the Aspin-Welch *t* test. Statistical significance was defined as * $P < .05$; ** $P < .01$.

Results

Characterization of $Cldn2^{-/-}$ and $Cldn15^{-/-}$ Small Intestines in Comparison With Wild Type

We compared the intestinal physiology of knockout mice for claudin-2 and claudin-15 because the luminal Na^+ -homeostasis is thought to be critical for small intestinal functions such as glucose absorption. First, we used immunofluorescence to examine the specific localization of claudin-2 and claudin-15 in the small intestines of wild-type mice. Consistent with previous studies,³⁶ the specific staining for claudin-2 and claudin-15 was confirmed by their disappearance in intestinal villi and crypts by each knockout (Figure 1A; Supplementary Figure 1A). In infant mice, claudin-2 was detected in the zTJs of the villi and crypts, but claudin-15 was expressed only in the zTJs of the crypts. Conversely, in the wild-type adult small intestine, claudin-15 was detected in the zTJs of the villi and crypts, but claudin-2 was expressed only in the crypts (Figure 1A and B; Supplementary Figure 1). Thus, we found age-dependent differences in the villous expression of claudin-2 and claudin-15, which were, respectively, expressed in the villi of infants and adults. Both claudins were detected in the crypts of infants and adults.

Macroscopically, at 2 weeks after birth, the small intestine of the $Cldn2^{-/-}$ mice was a little larger than that of their wild-type littermates (Figure 1C). Microscopically, the villi of the $Cldn2^{-/-}$ mice were slightly, but significantly, longer (at least in the proximal one-third of the small intestine) than in the wild-type small intestine (Figure 1B and D; Supplementary Figure 2), with no other obvious phenotypes in infants and adults (Supplementary Figure 2). These mild intestinal phenotypes in the $Cldn2^{-/-}$ mice were in sharp contrast to the prominent phenotypes in the $Cldn15^{-/-}$ mice, which showed a striking megaintestine phenotype in adults aged 8–16 weeks, as previously reported (Figure 1B–D; Supplementary Figure 1).³³

We next verified the patterns of distribution of claudin-2 and claudin-15 in the infant (2 weeks old) and adult (8–16 weeks old) knockout mice (Figure 1A; Supplementary Figure 1B); these patterns along with the wild-type patterns are depicted and categorized into types I–VI in Figure 1B. We found that the expression patterns of the other claudin family members (claudins-1/3/4/5/7/8/12/18/20/22/23) were not altered in the $Cldn2^{-/-}$ and $Cldn15^{-/-}$ mouse lines (Supplementary Figure 1B)³³ nor were altered expression levels detected for other cell adhesion-related proteins and transporters, such as Na^+/H^+ exchanger 3 (NHE3) (Supplementary Figures 3 and 4). In particular, we noted that, in the small intestine of $Cldn2^{-/-}$ infants (type II) and $Cldn15^{-/-}$ adults (type VI), the villi lacked both claudin-2 and claudin-15 (Figure 1A and B).

Deficiency of Claudin-2 or Claudin-15 Markedly Decreases the Transepithelial Conductance

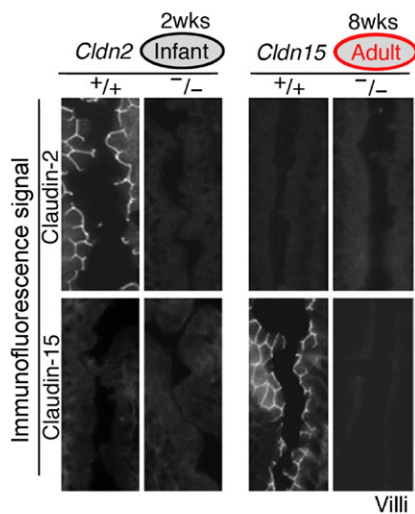
To examine the claudin-2- and claudin-15-based paracellular ion permeabilities, we first measured the electrical conductance across the small intestinal mucosa in wild-type, $Cldn2^{-/-}$, and $Cldn15^{-/-}$ infant (2 weeks old) and adult (8–16 weeks old) mice in an Ussing chamber system. For electrophysiologic measurements, the distal part of the middle one-third of the small intestine was used. The wild-type small intestine exhibited conductance values of 38.5 ± 2.6 mS/cm² in the infant mice (type I) and 27.1 ± 1.4 mS/cm² in the adult mice (type IV) (Figure 2A), thus meeting the criteria for electrophysiologically leaky epithelia, ie, higher than 1.0 mS/cm². In infant mice, the lack of claudin-2 or claudin-15 (type II or III) decreased the transepithelial conductance to 23.2 ± 1.4 mS/cm² or 23.3 ± 1.8 mS/cm², respectively. Thus, the claudin-15-based paracellular ion permeability in the crypts is comparable with the claudin-2-based paracellular ion permeability in both the villi and crypts in infants.

In adult mice, deficiencies in claudin-2 and claudin-15 (types V and VI) markedly decreased the transepithelial conductance to 22.1 ± 1.5 mS/cm² and 14.3 ± 1.0 mS/cm², respectively (Figure 2A). These results indicate that, because claudin-2 in the crypts and claudin-15 in the villi and crypts probably contributed to the paracellular permeabilities, the claudin-15-based paracellular ion permeability in the villi and crypts was much larger than that owing to claudin-2 expressed in the crypts in adults. These results are not consistent with the ones we obtained in infant mice, although the reason for the difference is unclear. However, at least a partial explanation lies in the difference in the total conductance across the small intestinal epithelia of infant vs adult mice.

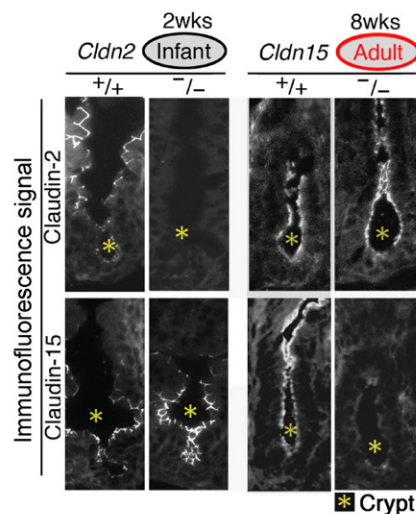
Deficiency of Claudin-2 or Claudin-15 Markedly Reduces the Selective Paracellular Permeability for Extracellular Monovalent Cations in the Small Intestine

Next, to determine the ion selectivities of the wild-type and knockout small intestinal epithelia, we measured the dilution potentials across the small intestinal mucosa under an apicobasal chemical gradient of NaCl (75 mmol/L NaCl at the apical side to 150 mmol/L NaCl at the basal side) and the ion selective ratio (P_{Na} vs P_{Cl}) was obtained (P_{Na} : permeability to Na^+ , P_{Cl} : permeability to Cl^-) (Figure 2B). When the dilution potentials were measured in both directions, the effects were symmetrical because of passive paracellular, rather than active transcellular, transport (Supplementary Figure 5A). Therefore, we replaced the apical solutions in most of our experiments. As calculated from the dilution potentials 8.1 ± 2.4 and 10.1 ± 1.8 mV (Figure 2C), respectively, (the basal side was defined as the zero reference) by the Goldman-Hodgkin-Katz equation, the ion selectivities ($P_{\text{Na}}/P_{\text{Cl}}$)

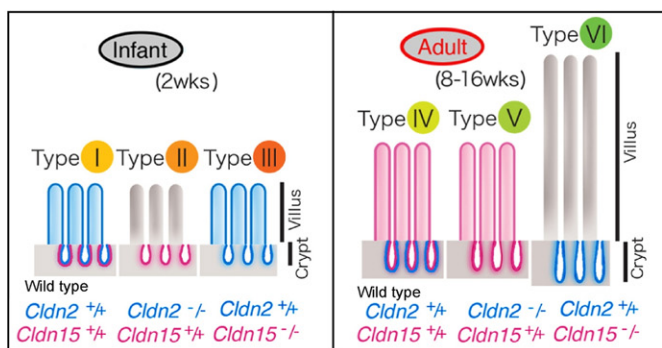
A Immunofluorescence (small intestinal villi)



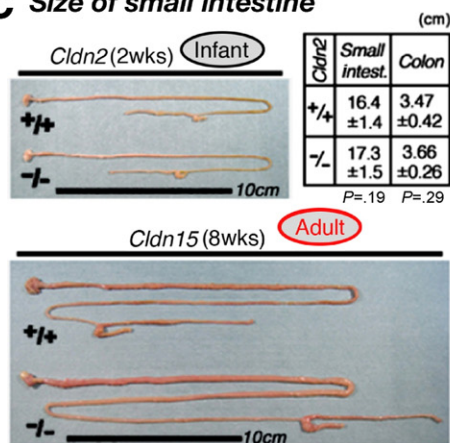
Immunofluorescence (small intestinal crypt)



B Expression of claudin-2 and claudin-15 in small intestine



C Size of small intestine



D Morphology of small intestine

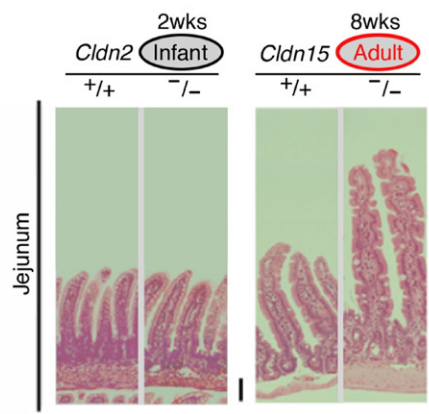


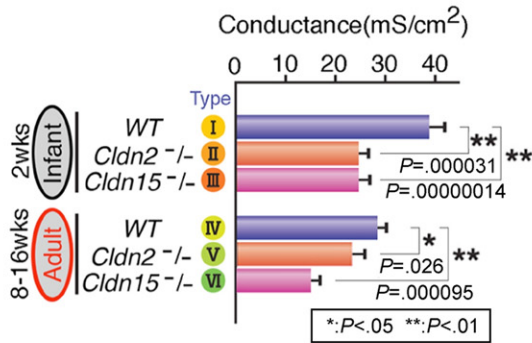
Figure 1. Characterization of the *Cldn2*^{-/-} and *Cldn15*^{-/-} small intestine. (A) Immunofluorescence signals for claudin-2 and claudin-15 in the small intestinal villi and crypts from *Cldn2*^{+/+} and *Cldn2*^{-/-} infant mice and *Cldn15*^{+/+} and *Cldn15*^{-/-} adult mice. Note that claudin-2 and claudin-15 are located at the belt-like tight junctions (zTJs) in the infant (2 weeks [2 wks]) and adult (8 weeks [8 wks]) small intestinal villi, respectively, although both are located at zTJs in crypts. Scale bar, 20 μ m. (B) Schematic drawings of the localizations of claudin-2 and claudin-15 in the infant (2 weeks [2 wks]) and adult (8–16 weeks [8–16 wks]) small intestines of wild-type, *Cldn2*^{-/-}*Cldn15*^{+/+}, and *Cldn2*^{+/+}*Cldn15*^{-/-} mice. Note the specific signals for claudin-2 and claudin-15 in the villi/crypts or crypts alone shown for the infant and adult mice. The expression patterns were divided into 6 types, identified as type I–type VI. (C) Macroscopic images of small intestines of 2-week-old *Cldn2*^{-/-} (infant) mice and 8-week-old *Cldn15*^{-/-} (adult) mice and their age-matched wild-type littermates. The table shows the intestinal lengths for the 2-week-old *Cldn2*^{-/-} (*n* = 7) and wild-type mice (*n* = 14). (D) H&E-stained intestinal villi from *Cldn2*^{+/+} and *Cldn2*^{-/-} infant and *Cldn15*^{+/+} and *Cldn15*^{-/-} adult mice. Scale bars, 50 μ m.

were 3.2 ± 1.1 in the wild-type infant intestine (type I) and 6.2 ± 1.9 in the wild-type adult intestine (type IV) (Figure 2D).

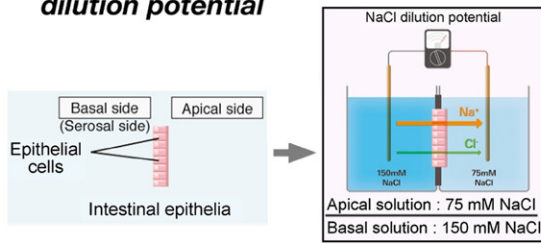
A deficiency in claudin-2 (types II and V) or claudin-15 (types III and VI) significantly lowered the NaCl-dilution potential in infant and adult mice, although to different

extents (Figure 2D). When P_{Na} and P_{Cl} were calculated independently (Figure 2E and F), the results showed that most of the Na⁺-selective paracellular permeability of the small intestine (Figure 2E), but not the Cl⁻-selective permeability (Figure 2F), was dependent on both claudin-2 and claudin-15. Hence, we concluded that clau-

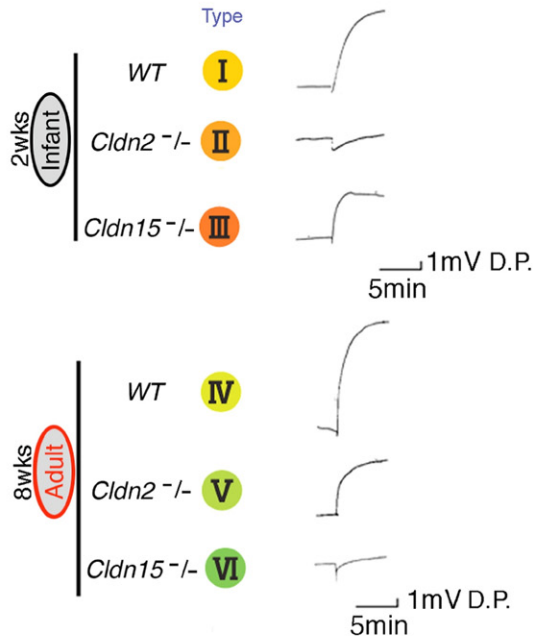
A Transepithelial conductance



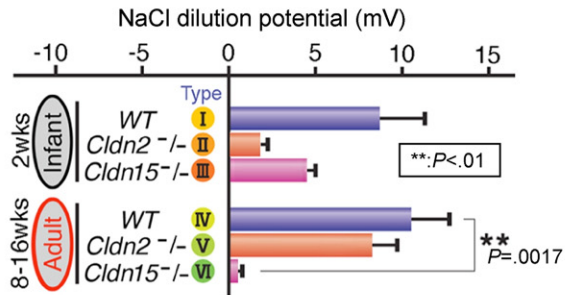
B Paracellular permeability for NaCl: indicated by dilution potential



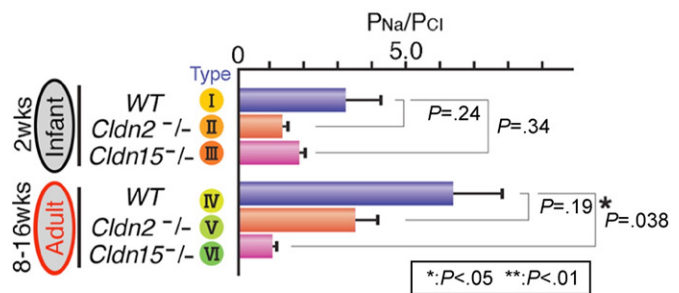
Apical soln. : 150mM NaCl 75mM NaCl
Basal soln. : 150mM NaCl 150mM NaCl



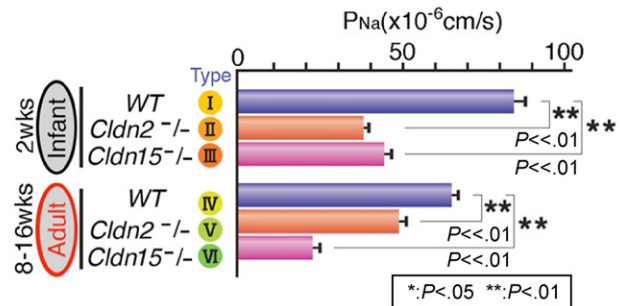
C Paracellular permeability for NaCl



D Ratio of paracellular permeability for Na⁺ and Cl⁻



E Na⁺ paracellular permeability



F Cl⁻ paracellular permeability

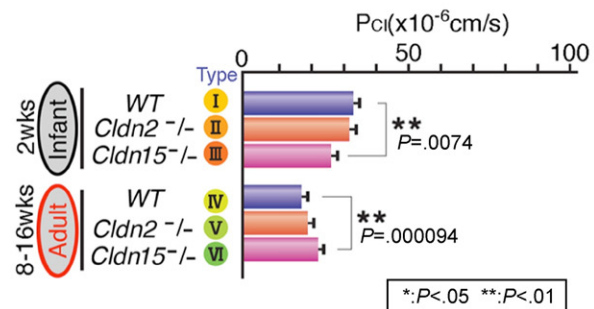


Figure 2. Electrophysiologic analyses of the roles of claudin-2 and claudin-15. (A) Statistical analyses of the ionic conductances across the small intestine of wild-type (WT), *Cldn2*^{-/-}, and *Cldn15*^{-/-} mouse infants (2 weeks [2 wks]) and adults (8–16 weeks [8–16 wks]) (n = 4–16). (B) Representative electrophysiologic measurements. Note the differences in dilution potentials in the small intestine of 2-week-old *Cldn2*^{-/-} infant mice and 8-week-old *Cldn15*^{-/-} adult mice compared with wild type. (C) Transepithelial NaCl dilution potentials across the small intestine of wild-type, *Cldn2*^{-/-}, and *Cldn15*^{-/-} infant and adult mice. Transepithelial dilution potentials were determined by the apical substitution of 150 mmol/L NaCl with 75 mmol/L NaCl. The osmolality was adjusted with mannitol (n = 3 or 4). (D) Statistical analyses of *P*_{Na}/*P*_{Cl} in the small intestine of *Cldn2*^{-/-} infant (2 weeks [2 wks]) and *Cldn15*^{-/-} adult (8–16 weeks [8–16 wks]) mice and their wild-type littermates. *P*, Permeability. The values were derived from the dilution potentials, which were calculated using the Goldman–Hodgkin–Katz equation (n = 3 or 4). (E and F) Statistical analyses of the *P*_{Na} (E) and *P*_{Cl} (F) values, respectively, for wild-type, *Cldn2*^{-/-}, and *Cldn15*^{-/-} intestines in infant and adult mice.

din-2 and claudin-15 contribute prominently to the Na^+ -selective transepithelial paracellular permeability and characterized them as intestinal “ Na^+ -leaky” claudins.

We next determined the permeabilities of the adult and infant small intestines of wild-type, *Cldn2*^{-/-}, and *Cldn15*^{-/-} mice for various monovalent cations. The results indicated that claudin-2 and claudin-15 are responsible for the paracellular channel-like permeability of monovalent cations, with the general rank of $\text{K}^+ \geq \text{Rb}^+ \geq \text{Cs}^+ > \text{Na}^+ > \text{Li}^+$ (Figure 3 and Supplementary Figure 5B and C). In adult mice, the paracellular permeability of monoionic cations was more highly dependent on clau-

din-15 (Figure 3D–F) than on claudin-2, compared with that in infant mice (Figure 3A–C). Because Na^+ is the dominant extracellular ion in the body (Supplementary Figure 6), the claudin-2- and claudin-15-based paracellular Na^+ -permeability in the small intestine was particularly noteworthy.

To confirm that the monovalent cation channel-like permeability was mediated by claudin-2 and claudin-15, we next determined the transepithelial (transmural) leakage of Na^+ and K^+ from the inside of an inverted small intestine in wild-type and *Cldn15*^{-/-} adult mice, into an external Na^+/K^+ -free mannitol solution, by measuring

Ion selectivity for various cations

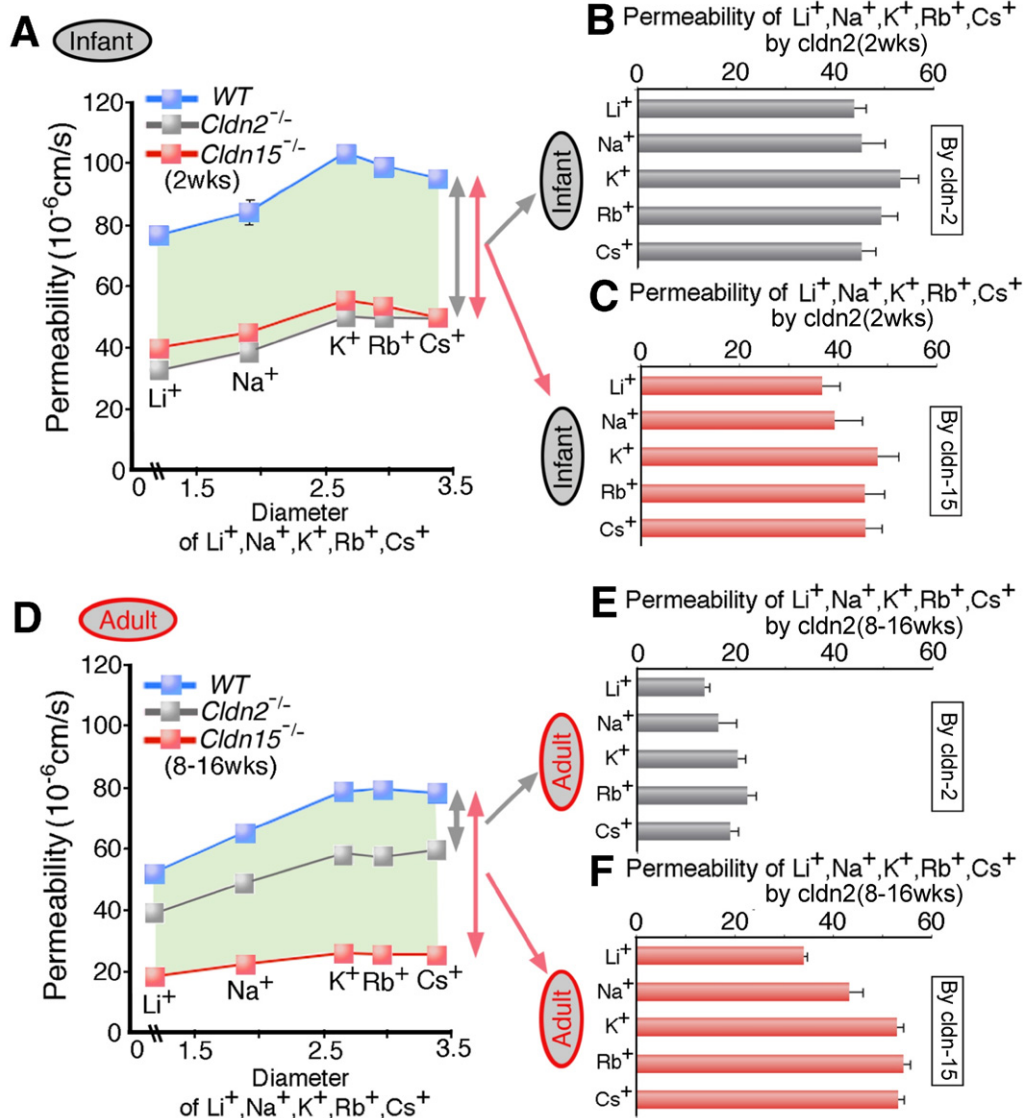


Figure 3. Transepithelial ion permeability ratios of the small intestine for various monovalent cations. To characterize the paracellular permeabilities attributable to claudin-2 and claudin-15, permeability for the monovalent cations Na^+ , Li^+ , K^+ , Rb^+ , and Cs^+ was determined. Calculations were based on the dilution potentials and performed using the Goldman–Hodgkin–Katz equation for the wild-type, *Cldn2*^{-/-}, and/or *Cldn15*^{-/-} small intestine of infant (2 weeks [2 wks]) (A–C) and adult (8–16 weeks [8–16 wks]) (D–F) mice. The difference in transcellular permeabilities between the wild-type and *Cldn2*^{-/-} or between the wild-type and *Cldn15*^{-/-} small intestine indicate the claudin-2- or claudin-15-dependent permeabilities for various ions, respectively.

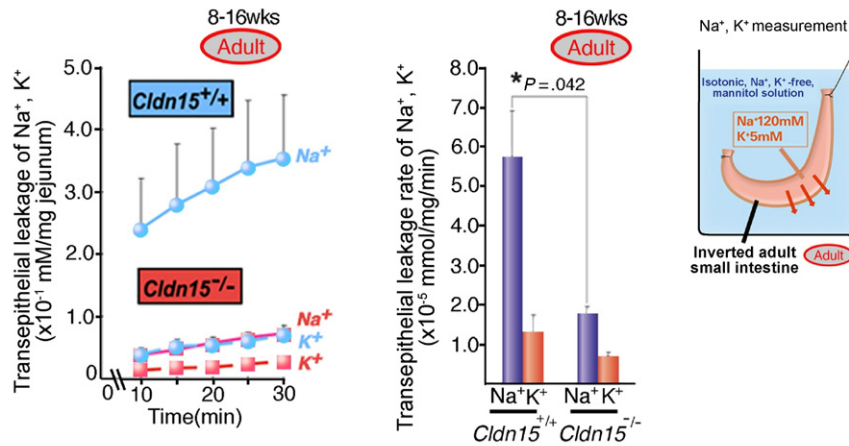
the Na⁺ and K⁺ concentrations in external solution (Figure 4A). The infant small intestine was too fragile to be used in this assay. The ends of the inverted adult intestine were tied to segregate the duodenum and ileum from the analysis. The leakage rates of Na⁺ and K⁺ (per milligram small intestine) from the inverted small intestine were markedly reduced in the *Cldn15*^{-/-} mice compared with wild-type (Figure 4A). Given that P_K/P_{Na} was >1.0 (Supplementary Figure 5B) and that the K⁺ leakage rate was much higher than the Na⁺ leakage rate (Figure 4A), the extracellular Na⁺ in the body (Supplementary Figure 6) may determine the Na⁺/K⁺ equilibrium.

Loss of Claudin-15, but not Claudin-2, Disturbs the Luminal Homeostasis of the Adult Small Intestine

We next examined the contributions of claudin-2 and claudin-15 to the luminal Na⁺-homeostasis of the

small intestine in vivo, which is particularly important because luminal Na⁺ is required for the absorption of nutrients such as glucose. To examine the Na⁺-homeostasis of the small intestine, we directly measured the luminal [Na⁺] and [K⁺] in vivo by sampling the small intestinal contents of wild-type, *Cldn2*^{-/-}, and *Cldn15*^{-/-} infant and adult mice (Figure 4B). In infants, the luminal [Na⁺] and [K⁺] showed wide variation, suggesting that the small intestinal luminal ionic homeostasis was not tightly regulated, partly because of the high total trans-epithelial conductance. In adults, the intestinal contents from the duodenum, jejunum, and ileum were collected separately. The luminal [Na⁺] and [K⁺] of the *Cldn15*^{-/-}, but not the *Cldn2*^{-/-}, adult small intestine were significantly different from wild type (Figure 4B). The *Cldn15*^{-/-} adult jejunum (type VI) contained 7.9 ± 0.5 mmol/L Na⁺ and 58.2 ± 1.3 mmol/L K⁺, which were

A Transepithelial permeability of Na⁺ and K⁺



B Luminal Na⁺ and K⁺ homeostasis

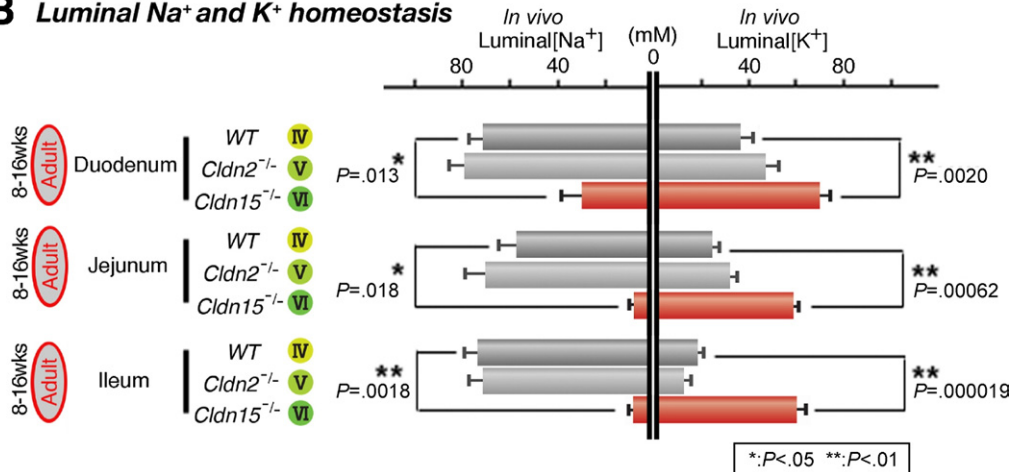


Figure 4. Paracellular permeabilities of Na⁺ and K⁺ and the in vivo intestinal homeostasis of Na⁺ in the small intestine of *Cldn15*^{-/-} adult mice and their wild-type littermates. (A) Measurements of the paracellular permeabilities of Na⁺ and K⁺ ions in the inverted small intestine of wild-type (WT) and *Cldn15*^{-/-} mice. (A, left) Time course of [Na⁺] and [K⁺] leakage from the inside of the small intestine from wild-type and *Cldn15*^{-/-} mice (n = 3 or 4). (A, middle) Leakage rate of Na⁺ and K⁺ from the inside of wild-type and *Cldn15*^{-/-} adult small intestine (n = 3 or 4). (A, right) Drawing of the experimental setup for an inverted small intestine. (B) [Na⁺] and [K⁺] in vivo in the intestinal content of wild-type and *Cldn2*^{-/-} and *Cldn15*^{-/-} adult mice. Note the drastic difference in ionic composition between the wild-type and *Cldn15*^{-/-} mouse small intestine (n = 4–11).

significantly different from the wild-type (type IV) values (57.2 ± 10.5 mmol/L Na^+ and 22.5 ± 3.4 mmol/L K^+) (Figure 4B). The claudin-2 deficiency in the adult small intestine did not disturb the luminal $[\text{Na}^+]$ or $[\text{K}^+]$, probably in part because the expression of claudin-2 was restricted to the crypts (type V) and in part because claudin-2 and claudin-15 may play different roles in establishing the properties of the paracellular channel-like ion permeability. Furthermore, in the colon, the same tendency was detected, possibly because of the influence of the small intestinal ionic condition. Although the expression of claudin-2 is reportedly higher in the colon,³⁶ the *Cldn2*^{-/-} adult colon showed a similar Na^+/K^+ balance as the wild-type one (Supplementary Figure 7). Therefore, the maintenance of ionic homeostasis in the adult intestine was highly dependent on the Na^+ -selectivity of claudin-15.

Loss of Claudin-15 Affects the Efficiency of Glucose Absorption Owing to the Lack of Small Intestinal Luminal Na^+

Based on our findings, it was likely that the Na^+ that leaked from the submucosa into the intestinal lumen through a claudin-15-based paracellular route provides the Na^+ required for the Na^+ -dependent absorption of nutrients such as glucose. In support of this idea, we recovered much more unabsorbed glucose from the small intestine of *Cldn15*^{-/-} mice than wild-type ones (Figure 5A), indicating that the loss of claudin-15 affected glucose absorption.

Next, to examine the effect of claudin-15-deficiency on glucose absorption in vivo, we carried out an OGTT by administering 2 or 1.5 grams D-glucose per kilogram body weight to the mice adults or infants, respectively (Figure 5B).⁴⁰ After the glucose administration, the time to the peak blood glucose level was significantly delayed in the *Cldn15*^{-/-} adult mice (30 minutes), but not in the *Cldn2*^{-/-} adult mice (15 minutes), compared with wild-type (15 minutes) (Figure 5B). Furthermore, in the *Cldn15*^{-/-} mice, the maximum blood glucose level was significantly lower than in the wild-type mice. The insulin level in the *Cldn15*^{-/-} mice was lower than in wild type during the OGTT (Figure 5B). Furthermore, the IPGTT did not show a delay in the peak blood glucose level of the *Cldn15*^{-/-} mice compared with wild type (Supplementary Figure 8A). There were no differences in OGTT among the infant wild-type, *Cldn2*^{-/-}, and *Cldn15*^{-/-} mice, which all showed the peak value of plasma glucose 30 minutes after glucose administration (Supplementary Figure 8B). In the adults, there was no difference detected in OGTT between wild-type and *Cldn2*^{-/-} adult mice, which both showed the peak value of plasma glucose 15 minutes after glucose administration (Figure 5B). Taken together, these data indicate that the *Cldn15*^{-/-}-associated delay in peak blood glucose in the OGTT occurred because the lack of luminal claudin-15 led to abnormally

low luminal Na^+ and consequently to impaired glucose absorption. Moreover, the *Cldn15*^{-/-} mice show a megaintestine phenotype, which may compensate to some extent for the defects in glucose absorption efficiency caused by the loss of claudin-15, suggesting that our evaluation of the effect of claudin-15 loss on glucose absorption per cell from the OGTT may be an underestimate.

To characterize the lack of glucose absorption efficiency in the *Cldn15*^{-/-} mice electrophysiologically, we examined the glucose-induced, SGLT1-based phlorizin-inhibited Isc in wild-type small intestine using Ussing chambers. When the luminal Na^+ concentration was 32 mmol/L, similarly to that of *Cldn15*^{-/-} duodenum, the glucose absorption was maintained at ~40% of the level seen with 72 mmol/L Na^+ , a similar value to that of wild-type intestine. However, the glucose absorption was decreased to <20% of this level when the luminal Na^+ concentration was 8 mmol/L similarly to that of jejunum and ileum (Figure 5C). These results suggested that, in the *Cldn15*^{-/-} small intestine, glucose absorption was decreased drastically in the jejunum and ileum, very consistent with the OGTT results, because the main site of glucose absorption is generally thought to be the jejunum and upper ileum.

Discussion

Our current results show that claudin-2 and claudin-15 function as paracellular monovalent cation-selective pores at zTJs and thereby mediate the long known but molecularly undefined high paracellular permeability to Na^+ and K^+ in the small intestinal epithelium. This permeability permits Na^+ , the main submucosal extracellular ion, access to the lumen to support the Na^+ -dependent absorption of nutrients. The permeability to K^+ is higher than to Na^+ , most likely to maintain the ionic balance with a high luminal concentration of Na^+ . In this context, the low permeability to Cl^- through the claudin-2- and claudin-15-regulated pores may be important for preventing too much NaCl (and water) from accumulating in the lumen. Figure 5D shows our hypothetical scheme for the claudin-15-based Na^+ -homeostasis of the adult small intestine and the effects on glucose absorption. Our findings, and the model, indicate that the transepithelial paracellular ion permeation system in the small intestine is quite sophisticated and optimized for the absorption of nutrients that require small intestinal luminal Na^+ , eg, glucose, amino acids, and vitamin C.^{1,3,4}

In the small intestine, the expression patterns of claudin-2 and claudin-15 change in an age-dependent way, as schematically shown in Figure 1B, consistent with a previous report.³⁶ In the infant small intestine (type I-type III), our electrophysiologic results suggested that the cryptic claudin-15 contributed about equally with the villous/cryptic claudin-2 to the transepithelial conductance. Given that our qRT-PCR results (Supplementary

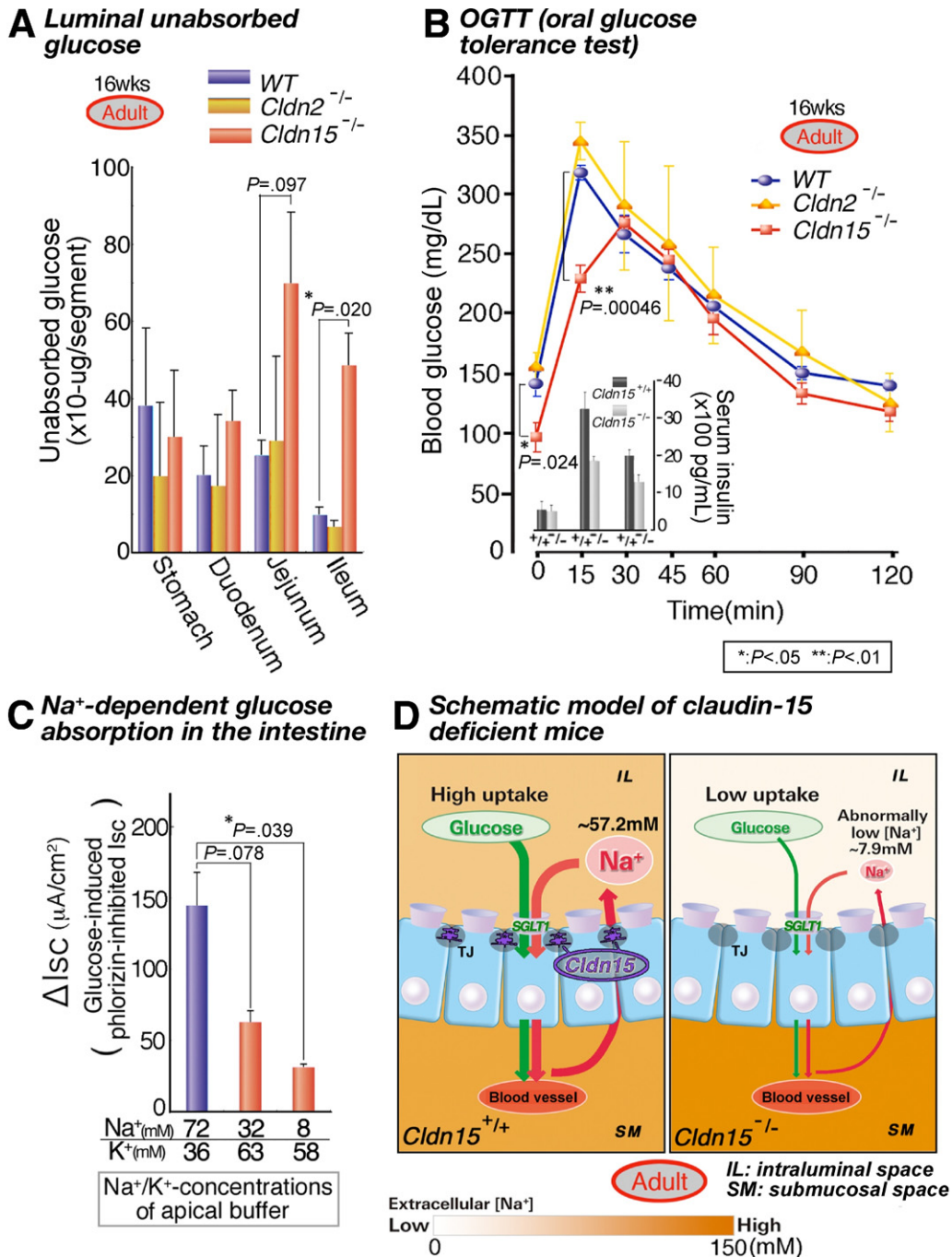


Figure 5. Claudin-15-dependent glucose absorption and model for the relationship between paracellular Na⁺ transport and glucose absorption in the small intestine and their dependence on claudin-15. (A) Unabsorbed glucose content in the wild-type, *Cldn2*^{-/-}, and *Cldn15*^{-/-} adult small intestine (n = 3 or 4). (B) A 2-g/kg body weight oral glucose tolerance test in wild-type, *Cldn2*^{-/-}, and *Cldn15*^{-/-} adult mice (n = 3–6), showing the absorption of glucose. Serum insulin level was also measured in *Cldn15*^{-/-} adult mice. (C) Na⁺-dependent glucose absorption as determined by ΔIsc. Isc, short circuit current. Apical sides of the Ussing chambers of wild-type mouse duodenum and jejunum were bathed with buffers (osmolality was maintained with mannitol equal to basal solution) containing Na⁺/K⁺ concentrations similar to the luminal ionic ones of duodenum and jejunum in vivo, respectively. [Na⁺]-dependent glucose absorption was assessed by the increase in Isc (ΔIsc) owing to mucosal addition of 10 mmol/L D-glucose in wild-type adult mice jejunum in each condition (n = 3). Note the dramatic decrease of ΔIsc in low Na⁺-condition, similar to one of the *Cldn15*^{-/-} jejunum and ileum. (D) Schematic drawing showing the relationship between the claudin-15-dependent paracellular Na⁺ permeability and glucose absorption in the small intestine. The relative amount of paracellular Na⁺ leakage across the paracellular tight junction (TJ) is indicated by the size of each arrow, and the relative amount of glucose absorbed is also indicated by the size of the arrow. The luminal and submucosal Na⁺ concentration ([Na⁺]) is indicated by color between 0 mmol/L (Low) and 150 mmol/L (High) and by the size of the lettering. Note the difference in [Na⁺] between wild-type *Cldn15*^{+/+} (left) and *Cldn15*^{-/-} (right) adult mice. In adults, the relatively high [Na⁺] in the submucosa of the *Cldn15*^{-/-} small intestine is thought to be obtained because the secretion of Na⁺ into the lumen is retarded by the absence of claudin-15, which plays a role in the paracellular Na⁺ channel-like permeability. Thus, the deficiency of claudin-15 decreases the luminal [Na⁺] and subsequently decreases the absorption of glucose by Na⁺-driven transporters in *Cldn15*^{-/-} adult mice (right).

Figure 1B) showed that the claudin-2 level was higher than that of claudin-15 in the infant small intestine, cryptic claudin-15 must contribute more to the ion permeability than cryptic/villous claudin-2. However, claudin-2 showed a greater selectivity for monovalent cations than cryptic claudin-15, as revealed by the dilution potential and the bi-ionic potential for Na⁺ and other monovalent cations (Figure 2C and Figure 3). That is, the claudin-2-based paracellular permeability carries a smaller current and is highly selective for Na⁺, when localized in the villi and crypts, compared with the cryptic claudin-15-based permeability. However, the ionic homeostasis of the *Cldn2*^{-/-} and *Cldn15*^{-/-} infant small intestine was not critically disturbed (Supplementary Figure 7).

In the adult, we compared the *Cldn15*^{-/-} (type VI in Figure 1B) and *Cldn2*^{-/-} (type V) small intestine with wild type (type IV). Our analyses suggested that the villous/cryptic claudin-15 contributed more to both the total conductance and the selectivity for monovalent cations than did the cryptic claudin-2. Our qRT-PCR analysis showed that the expression level of claudin-15 was much higher than that of claudin-2 in the adult small intestine (Supplementary Figure 1B), which was consistent with the differences in the permeability and ion selectivity we observed in the knockout mice. Hence, it is possible that the claudin-2- and/or claudin-15-based paracellular ion channel-like permeabilities have different characteristics in the infant and adult small intestine and that their contributions may differ depending on their location at the villi and/or crypts. Hence, it is difficult to speculate based on the present study why the expression of claudin-2 in the infant intestinal villi changes to that of claudin-15 in the adult intestinal villi. It is noteworthy that the loss of claudin-15 induced aberrantly low concentrations of luminal Na⁺ in the adult small intestine. However, in the infant small intestine, in which claudin-15 expression is confined to the cryptic regions, it did not play a critical role in determining the luminal [Na⁺]. Hence, claudin-15 is the dominant determinant of Na⁺-homeostasis when it is localized in the villi of the adult small intestine.

Our OGTT results showed that the glucose absorption was largely impaired by a deficiency of microvillous claudin-15 in the adult intestine, which was confirmed by the IPGTT (Supplementary Figure 8A). The *Cldn15*^{-/-} megaintestine phenotype may compensate to some extent for the defects in the efficiency of glucose absorption caused by the loss of claudin-15, suggesting that our evaluation of the effect of the claudin-15 loss on glucose absorption per cell from the OGTT may be an underestimate. Because the insulin level of the *Cldn15*^{-/-} mice was lower than that of wild-type during the OGTT (Figure 5B)⁴⁰ and the maximum blood glucose level was significantly lower in *Cldn15*^{-/-} mice than in *Cldn15*^{+/+} mice even at the large intestine, the glucose absorption is probably impaired by the deficiency of claudin-15. It is

most likely that the decrease in luminal Na⁺ affected the SGLT1 in the *Cldn15*^{-/-} small intestine, particularly in the jejunum, which is thought to be the major site of glucose absorption, because the glucose-induced, phlorizin-inhibited Isc in the Ussing chambers was largely decreased in the wild-type jejunum under an Na⁺ concentration similar to that of the *Cldn15*^{-/-} jejunum (Figure 4B; Supplementary Figure 4C). Although NHE3 is thought to be regulated similarly to SGLT1 (similar K_{Na+}), no differences in the luminal pH between the wild-type and *Cldn15*^{-/-} jejunum were observed (Figure 4B), suggesting that the luminal pH is determined by more factors than NHE3. Thus, the claudin-2- and claudin-15-knockout mice may provide good model systems for examining the effects of these claudins in inflammatory bowel disease (IBD) because it has been suggested that increases in intestinal permeability and claudin-2 expression precede the onset of IBD^{41,42} and that at least claudin-15 and claudin-10 show increased expression in the hyperinflamed colon of JAM-A knockout mice, an IBD model,⁴³ although this point remains to be explored in future studies.

In conclusion, we used an experimental paradigm in which we disrupted the *in vivo* claudin-based ion permeability of the small intestine and examined its effect on glucose metabolism. Our findings are particularly important because they indicate that tight-junctional claudin-15 can regulate Na⁺-homeostasis and glucose metabolism, which is a novel finding. The systematic knockout of claudins in mice will shed light on the specific roles of these proteins throughout the body and in any observed claudin-related disorders caused by the specific deficiencies, which could lead to new medical treatments for paracellular permeability-related diseases.

Supplementary Material

Note: To access the supplementary material accompanying this article, visit the online version of *Gastroenterology* at www.gastrojournal.org, and at doi: 10.1053/j.gastro.2010.08.006.

References

- Schultz SG, Curran PF. Coupled transport of sodium and organic solutes. *Physiol Rev* 1970;50:637–718.
- Farhadi A, Banan A, Fields J, et al. Intestinal barrier: an interface between health and disease. *J Gastroenterol Hepatol* 2003;18:479–497.
- Kapus A, Szász K. Coupling between apical and paracellular transport processes. *Biochem Cell Biol* 2006;84:870–880.
- Tsukaguchi H, Tokui T, Mackenzie B, et al. A family of mammalian Na⁺-dependent L-ascorbic acid transporters. *Nature* 1999;399:70–75.
- Parsons DS. Sodium chloride absorption by the small intestine and the relationships between salt transport and the absorption of water and some organic molecules. *Proc Nutr Soc* 1967;26:46–54.
- Claude P, Goodenough DA. Fracture faces of zonulae occludentes from “tight” and “leaky” epithelia. *J Cell Biol* 1973;58:390–400.

7. Powell DW. Barrier function of epithelia. *Am J Physiol* 1981;241:G275–G288.
8. Wright EM. Diffusion potentials across the small intestine. *Nature* 1966;212:189–190.
9. Frizzell RA, Schultz SG. Ionic conductances of extracellular shunt pathway in rabbit ileum. Influence of shunt on transmural sodium transport and electrical potential differences. *J Gen Physiol* 1972;59:318–346.
10. Okada Y, Irimajiri A, Inouye A. Electrical properties and active solute transport in rat small intestine. II. Conductive properties of transepithelial routes. *J Membr Biol* 1977;31:221–232.
11. Madara JL. Regulation of the movement of solutes across tight junctions. *Annu Rev Physiol* 1998;60:143–159.
12. Tsukita S, Furuse M, Itoh M. Multifunctional strands in tight junctions. *Nat Rev Mol Cell Biol* 2001;2:285–293.
13. Van Itallie CM, Anderson JM. Claudins and epithelial paracellular transport. *Annu Rev Physiol* 2006;68:403–429.
14. González-Mariscal L, Lechuga S, Garay E. Role of tight junctions in cell proliferation and cancer. *Prog Histochem Cytochem* 2007;42:1–57.
15. Yu D, Turner JR. Stimulus-induced reorganization of tight junction structure: the role of membrane traffic. *Biochim Biophys Acta* 2008;1778:709–716.
16. Tsukita S, Yamazaki Y, Katsuno T, et al. Tight junction-based epithelial microenvironment and cell proliferation. *Oncogene* 2008;27:6930–6938.
17. Furuse M, Furuse K, Sasaki H, et al. Conversion of zonulae occludentes from tight to leaky strand type by introducing claudin-2 into Madin-Darby canine kidney I cells. *J Cell Biol* 2001;153:263–272.
18. Colegio OR, Van Itallie CM, McCrea HJ, et al. Claudins create charge-selective channels in the paracellular pathway between epithelial cells. *Am J Physiol* 2002;283:C142–C147.
19. Van Itallie CM, Fanning AS, Anderson JM. Reversal of charge. Selectivity in cation or anion-selective epithelial lines by expression of different claudins. *Am J Physiol* 2003;285:F1078–F1084.
20. Van Itallie CM, Anderson JM. The role of claudins in determining paracellular charge selectivity. *Proc Am Thorac Soc* 2004;1:38–41.
21. Hou J, Gomes AS, Paul DL, et al. Study of claudin function by RNA interference. *J Biol Chem* 2006;281:36117–36123.
22. Amasheh S, Meiri N, Gitter AH, et al. Claudin-2 expression induces cation-selective channels in tight junctions of epithelial cells. *J Cell Sci* 2002;115:4969–4976.
23. Yu AS, Cheng MH, Angelow S, et al. Molecular basis for cation selectivity in claudin-2-based paracellular pores: identification of an electrostatic interaction site. *J Gen Physiol* 2009;133:111–127.
24. Gow A, Southwood CM, Li JS, et al. CNS myelin and sertoli cell tight junction strands are absent in *Osp/claudin-11* null mice. *Cell* 1999;99:649–659.
25. Simon DB, Lu Y, Choate KA, et al. Paracellin-1, a renal tight junction protein required for paracellular Mg²⁺ resorption. *Science* 1999;285:103–106.
26. Wilcox ER, Burton QL, Naz S, et al. Mutations in the gene encoding tight junction claudin-14 cause autosomal recessive deafness DFNB29. *Cell* 2001;104:165–172.
27. Furuse M, Hata M, Furuse K, et al. Claudin-based tight junctions are crucial for the mammalian epidermal barrier: a lesson from claudin-1-deficient mice. *J Cell Biol* 2002;156:1099–1111.
28. Nitta T, Hata M, Gotoh S, et al. Size-selective loosening of the blood-brain barrier in claudin-5-deficient mice. *J Cell Biol* 2003;161:653–660.
29. Uyguner O, Emiroglu M, Uzumcu A, et al. Frequencies of gap- and tight-junction mutations in Turkish families with autosomal-recessive non-syndromic hearing loss. *Clin Genet* 2003;64:65–69.
30. Kang JH, Choi HJ, Cho HY, et al. Familial hypomagnesemia with hypercalciuria and nephrocalcinosis associated with CLDN16 mutations. *Pediatr Nephrol* 2005;20:1490–1493.
31. Thorleifsson G, Holm H, Edvardsson V, et al. Sequence variants in the CLDN14 gene associate with kidney stones and bone mineral density. *Nat Genet* 2009;41:926–930.
32. Miyamoto T, Morita K, Takemoto D, et al. Tight junctions in Schwann cells of peripheral myelinated axons: a lesson from claudin-19-deficient mice. *J Cell Biol* 2005;169:527–538.
33. Tamura A, Kitano Y, Hata M, et al. Megaintestine in claudin-15-deficient mice. *Gastroenterology* 2008;134:523–534.
34. Muto S, Hata M, Taniguchi J, et al. Claudin-2-deficient mice are defective in the leaky and cation-selective paracellular permeability properties of renal proximal tubules. *Proc Natl Acad Sci U S A* 2010;107:8011–8016.
35. Fujita H, Chiba H, Yokozaki H, et al. Differential expression and subcellular localization of claudin-7, -8, -12, -13, and -15 along the mouse intestine. *J Histochem Cytochem* 2006;54:933–944.
36. Holmes JL, Van Itallie CM, Rasmussen JE, et al. Claudin profiling in the mouse during postnatal intestinal development and along the gastrointestinal tract reveals complex expression patterns. *Gene Expr Patterns* 2006;6:581–588.
37. Turner JR. Intestinal mucosal barrier function in health and disease. *Nat Rev Immunol* 2009;9:799–809.
38. Saitou M, Furuse M, Sasaki H, et al. Complex phenotype of mice lacking occludin, a component of tight junction strands. *Mol Biol Cell* 2000;11:4131–4142.
39. Nishinaga H, Komatsu R, Doi M, et al. Circadian expression of the Na⁺/H⁺ exchanger NHE3 in the mouse renal medulla. *Biomed Res* 2009;30:87–93.
40. Miyawaki K, Yamada Y, Yano H, et al. Glucose intolerance caused by a defect in the entero-insular axis: a study in gastric inhibitory polypeptide receptor knockout mice. *Proc Natl Acad Sci U S A* 1999;96:14843–14847.
41. Hering NA, Schulzke JD. Therapeutic options to modulate barrier defects in inflammatory bowel disease. *Dig Dis* 2009;27:450–454.
42. Weber CR, Nalle SC, Tretiakova M, et al. Claudin-1 and claudin-2 expression is elevated in inflammatory bowel disease and may contribute to early neoplastic transformation. *Lab Invest* 2008;88:1110–1120.
43. Laukoetter MG, Nava P, Lee WY, et al. JAM-A regulates permeability and inflammation in the intestine in vivo. *J Exp Med* 2007;204:3067–3076.

Received May 5, 2010. Accepted August 9, 2010.

Reprint requests

Address requests for reprints to: Sachiko Tsukita, PhD, Laboratory of Biological Science, Graduate School of Frontier Biosciences and Graduate School of Medicine, Osaka University, 2-2 Yamadaoka, Suita, Osaka 565-0871, Japan. e-mail: atsukita@biosci.med.osaka-u.ac.jp; fax: (81) 6-6879-3329.

Acknowledgments

The authors thank the members of their laboratories and Drs Grace Gray and Leslie Miglietta for proofreading the manuscript.

This paper is dedicated to the late Dr Shoichiro Tsukita, who asked Tetsuo Noda and Sachiko Tsukita to keep and use the frozen embryos of the knockout mice to continue and develop the work he had intended.

Conflicts of interest

The authors disclose no conflicts.

Funding

Supported by a Grant-in-Aid for Creative the Scientific Research from the Ministry of Education, Science and Culture of Japan (to S.T.).